from 96 NSCLC specimens (Figs 2,S2). The prevalence of methylation among the 96 cases was 25.0% (24/96) for *mir-152*, 64.6% (62/96) for *mir-9-1*, 27.1% (26/96) for *mir-124-1*, 50% (48/96) for *mir-124-2*, and 50% (48/96) for *mir-124-3*. The frequency of methylation is shown according to the clinical features in Table 3. The methylation of *mir-124-2* and *mir-124-3* was similarly and preferentially observed in older patients or smokers. No significant correlations were seen between the methylation status of *mir-152* or *mir-124-1* and the clinicopathological features, whereas the methylation statuses of *mir-9-3, -124-2*, and *-124-3* were correlated with the T classification.

Risk of advanced pathological features according to CpG island methylation status of five miRNAs. To estimate the risk of advanced pathological features among the methylation statuses of the miRNA loci, compared with that among the unmethylated statuses, a multivariate logistic regression analysis was carried out (Table 4). The odds ratio for each miRNA locus was

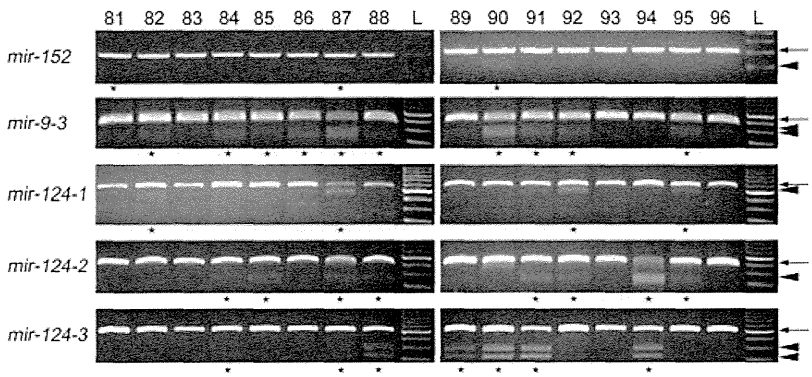

Fig. 2. Representative combined bisulfite restriction analysis results of non-small-cell lung carcinoma tissue samples. Arrows, unmethylated alleles; arrowheads, methylated alleles; L, DNA size markers; numbers on top, tissue samples; stars, samples with significant restricted fragments from methylated alleles.

Table 3. Relationships between CpG island methylation of miRNAs and clinicopathological features in 96 patients with non-small-cell lung carcinoma

Characteristics	Methylated locus									
	mir-152		*mir-9-3*		*mir-124-1*		*mir-124-2*		*mir-124-3*	
	n (%)	*P*	*n* (%)	*P*	*n* (%)	*P*	*n* (%)	*P*	*n* (%)	*P*
Overall (*n* = 96)	24 (25.0)	–	62 (64.6)	–	26 (27.1)	–	48 (50.0)	–	48 (50.0)	–
Age (years)										
≤65 (*n* = 47)	12 (25.5)	0.9062	26 (55.3)	0.0631	12 (25.5)	0.7376	16 (34.0)	0.0022*	18 (38.3)	0.0247*
>65 (*n* = 49)	12 (24.5)	–	36 (73.5)	–	14 (28.6)	–	32 (65.3)	–	30 (61.2)	–
Sex										
Male (*n* = 60)	18 (30.0)	0.1441	40 (66.7)	0.5816	17 (28.3)	0.722	34 (56.7)	0.0917	33 (55.0)	0.2059
Female (*n* = 36)	6 (16.7)	–	22 (61.1)	–	9 (25.0)	–	14 (38.9)	–	15 (41.7)	–
Smoking habit										
Never (*n* = 33)	6 (18.2)	0.2642	20 (60.6)	0.5554	8 (24.2)	0.6503	11 (33.3)	0.0181*	11 (33.3)	0.0181*
Ever (*n* = 63)	16 (25.4)	–	42 (66.7)	–	18 (28.6)	–	37 (58.7)	–	37 (58.7)	–
Histological type										
Adenocarcinoma (*n* = 78)	22 (28.2)	0.2253	52 (66.7)	0.3743	24 (30.8)	0.1402	36 (46.2)	0.1167	36 (46.2)	0.1167
Others (*n* = 18)	2 (11.1)	–	10 (55.6)	–	2 (11.1)	–	12 (66.7)	–	12 (66.7)	–
Stage										
IA, IB (*n* = 67)	20 (29.9)	0.0953	42 (62.7)	0.5548	19 (28.4)	0.6692	31 (46.3)	0.2664	33 (49.3)	0.8241
IIA–IIIA (*n* = 29)	4 (13.8)	–	20 (69.0)	–	7 (24.1)	–	17 (58.6)	–	15 (51.7)	–
T factor										
T1 (*n* = 54)	11 (20.4)	0.2349	29 (53.7)	0.0115*	12 (22.2)	0.2243	20 (37.0)	0.0040*	19 (35.2)	0.0010*
T2 (*n* = 42)	13 (31.0)	–	33 (78.6)	–	14 (33.3)	–	28 (66.7)	–	29 (69.0)	–
N factor										
Negative (*n* = 67)	20 (29.9)	0.0953	42 (62.7)	0.5548	19 (28.4)	0.6692	31 (46.3)	0.2664	33 (49.3)	0.8241
Positive (*n* = 29)	4 (13.8)	–	20 (69.0)	–	7 (24.1)	–	17 (58.6)	–	15 (51.7)	–
Lymphatic invasion										
Negative (*n* = 72)	18 (25.0)	1.0000	44 (61.1)	0.2179	19 (26.4)	0.7909	34 (47.2)	0.3458	33 (45.8)	0.1573
Positive (*n* = 24)	6 (25.0)	–	18 (75.0)	–	7 (29.2)	–	14 (58.3)	–	15 (62.5)	–
Vascular invasion										
Negative (*n* = 58)	15 (25.9)	0.8096	36 (62.1)	0.5245	15 (25.9)	0.7394	27 (46.6)	0.4038	28 (48.3)	0.6764
Positive (*n* = 38)	9 (23.7)	–	26 (68.4)	–	11 (28.9)	–	21 (55.3)	–	20 (52.6)	–
EGFR mutation										
Negative (*n* = 65)	15 (23.1)	0.3077	42 (64.6)	0.5949	17 (26.2)	0.7329	38 (58.5)	0.0118*	36 (55.4)	0.2007
Positive (*n* = 27)	9 (33.3)	–	19 (70.4)	–	8 (29.6)	–	8 (29.6)	–	11 (40.7)	–

*$P < 0.05$. EGFR, epidermal growth factor receptor; *n*, number of cases.

doi: 10.1111/j.1349-7006.2011.02101.x

adjusted for age, sex, and smoking habit. The methylation status of *mir-9-3, -124-2*, and *-124-3* were significantly associated with the T factor. When *mir-9-3, -124-2*, or *-124-3* was methylated, the adjusted odds ratio for a T2 status was 3.11 (95% CI, 1.26–8.22; $P = 0.0130$), 3.39 (95% CI, 1.39–8.67; $P = 0.0066$), or 4.17 (95% CI, 1.69–10.89; $P = 0.0017$), respectively. The status of at least two methylated miRNA loci was also examined to determine the association with advanced pathological features. When the methylation of two or more miRNA loci was observed, the estimated odds ratio for a T2 status was 4.75 (95% CI, 1.83–13.59; $P = 0.0011$).

Kaplan–Meier estimates. The 5-year PFS of the cohort was 67%. In a univariate analysis of the known clinicopathological risk factors, the T classification was the most significant prognostic factor. Patients with a T2 status had a significantly lower PFS ($P < 0.0001$), compared with those with T1 disease (Fig. 3A). The presence of at least two methylated miRNA loci, which was shown to be a strong predictor of a T2 status, was also a significant predictor of a poor PFS in a univariate analysis ($P = 0.0177$, Fig. 3B).

Discussion

Our study showed that the CpG island methylation of *mir-152* was common in NSCLC clinical specimens. The prevalence was 25%. However, no correlation was seen between the methylation status of *mir-152* and clinicopathological features. The methylation of *mir-152* was reportedly associated with an advanced tumor stage and a poorer PFS in patients with bladder cancer.[17] The regulation of miRNAs is believed to be highly tissue specific;[18] thus, the role of *miR-152*, if any, may not be dominant in lung cancer.

Our results showed that the methylated status of *mir-9-3* was a significant risk factor for an advanced T status in a multivariate regression analysis. In contrast, no correlation was seen between the methylation of *mir-9-3* and pathological parameters other than the T classification. The methylation of *mir-9-3* has been reported in a wide range of primary tumors, such as colorectal, head and neck, breast, and lung cancers, and melanoma.[11,19] Lujambio *et al.*[11] reported the frequency of methylation in lung cancer to be 53%, and the methylation of *mir-9-3* was associated with lymph node metastasis. Although we observed a similar proportion of methylated *mir-9-3*, no correlation was seen between the methylation of *mir-9-3* and lymph node metastasis in our cohort. This discrepancy may be explained by inconsistencies between the patient cohorts, as the characteristics of the patients were not described in the previous report. Other possible reasons could include the methods used to detect methylation (i.e. methylation-specific PCR versus COBRA), or the precise CpG site targeted for analysis by these methods.

One remarkable finding regarding *miR-124* was that *mir-124-2* and *mir-124-3* showed similar methylation profiles that were distinct from that of *mir-124-1* (Table 3, Fig. S2), even though *mir-124-2* and *mir-124-3* are on separate chromosomes (8q12 and 20q13, respectively). The methylation of *miR-124* has been

Table 4. Multivariate odds ratios (OR) and 95% confidence intervals (CI) for the estimated risk of advanced pathological findings in non-small-cell lung cancer specimens according to miRNA methylation status

Category	T factor (T2 *vs* T1)		N factor (Positive)		Lymphatic invasion (Positive)		Vascular invasion (Positive)	
	OR† (95%CI)	*P*	OR† (95%CI)	*P*	OR† (95%CI)	*P*	OR† (95%CI)	*P*
mir-152								
Unmethylated	1.00	–	1.00	–	1.00	–	1.00	–
Methylated	1.76 (0.67–4.68)	0.2428	0.35 (0.09–1.09)	0.0719	1.04 (0.32–3.02)	0.9432	0.76 (0.27–1.99)	0.5815
mir-9-3								
Unmethylated	1.00	–	1.00	–	1.00	–	1.00	–
Methylated	3.11 (1.26–8.22)	0.0130*	1.36 (0.53–3.72)	0.5212	1.77 (0.64–5.45)	0.2766	1.38 (0.57–3.48)	0.4717
mir-124-1								
Unmethylated	1.00	–	1.00	–	1.00	–	1.00	–
Methylated	1.69 (0.67–4.29)	0.2591	0.80 (0.27–2.18)	0.6801	1.08 (0.36–2.97)	0.8776	1.18 (0.45–3.05)	0.7215
mir-124-2								
Unmethylated	1.00	–	1.00	–	1.00	–	1.00	–
Methylated	3.39 (1.39–8.67)	0.0066*	1.98 (0.76–5.47)	0.1632	1.43 (0.53–3.94)	0.4766	1.37 (0.56–3.42)	0.4815
mir-124-3								
Unmethylated	1.00	–	1.00	–	1.00	–	1.00	–
Methylated	4.17 (1.69–10.89)	0.0017*	1.25 (0.48–3.33)	0.6371	1.84 (0.68–5.21)	0.2290	1.12 (0.45–2.76)	0.7995
0 or 1 methylated locus	1.00	–	1.00	–	1.00	–	1.00	–
2 or more methylated loci	4.75 (1.83–13.59)	0.0011*	0.99 (0.38–2.68)	0.9994	1.98 (0.69–6.27)	0.2021	1.59 (0.63–4.11)	0.3222

*$P < 0.05$. †Odds ratios are reported on the basis of a multivariate logistic regression model adjusted for age, sex, and smoking habit.

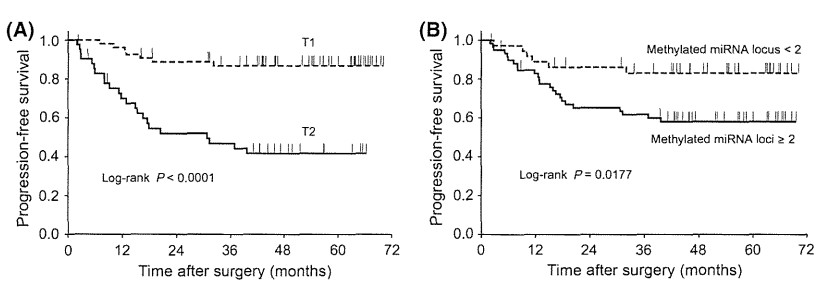

Fig. 3. (A) Kaplan–Meier analysis of progression-free survival among 96 non-small-cell lung carcinoma patients according to T classification. (B) Kaplan–Meier analysis of progression-free survival among 96 non-small-cell lung carcinoma patients, according to the number of methylated loci.

reported in various tumor types including colon, breast, lung, and hepatocellular carcinomas, leukemias, and lymphomas.[10,20,21] However, whether the methylation of *miR-124* occurs independently or coordinately remains uncertain.

The methylation of the promoter regions of certain protein-coding genes is reportedly associated with poor clinical outcomes in lung cancer.[22–24] A subset of the CpG island methylator phenotype (CIMP), originally established in colorectal carcinoma,[25,26] is characterized by the synchronous hypermethylation of multiple promoter CpG island regions and peculiar clinicopathological findings. Although several reports have indicated that CIMP is also distinguishable in NSCLC and is associated with a poor prognosis,[27,28] we have failed to distinguish the phenotype in the previous study regarding the methylation of the promoter regions of numerous protein-coding genes.[29] In the present study, we analyzed whether the concordant hypermethylation of multiple miRNA loci results in characteristics similar to those of CIMP. The methylated status of two or more miRNA loci was found to be associated with a significantly higher risk for advanced T status independent of age, sex, and smoking habit. Moreover, the methylation of multiple miRNA loci was associated with a poorer PFS.

Whether the aberrant methylation that occurs in cancer is a cause or a consequence is a difficult question.[30] The tumor size of NSCLC can be assumed to reflect the number of cancer cell divisions that have occurred since the initiation of carcinogenesis. However, the pathological findings of lymph node metastases or vessel invasions may be regarded as traits that have acquired a certain aggressive character at some point in time. Our result that only the T factor was associated with miRNA methylation suggests that the methylation of individual miRNA loci did not trigger any drastic phenotypic change in the NSCLCs and that what we observed was the accumulation of DNA methylation events during tumor progression. Indeed, according to the neutral theory of molecular evolution established in population biology,[31] it is most natural to suppose that the great majority of somatic mutations or aberrant methylations observed in cancer are neutral with regard to phenotypic alterations. Alterations that truly disrupted the cell cycle and affected the cell phenotype would be lethal for those cells, and such cells would probably not be visible in the tissue specimens.

In the present study, we did not carry out an expression analysis of miRNAs. Degrading of RNAs is inevitable during the sample preparation. Moreover, detecting suppression of aberrantly methylated genes is vulnerable to minimal contamination of highly expressed transcripts in the normal tissues. In this concern, detecting the accumulation of DNA methylation in the promoter region is one of the simplest and most consistent approaches to looking at the natural course of carcinogenesis, and our concept of focusing on a small number of examined loci among a small miRNA population (less than one-tenth of the protein coding genes) has the advantages of being cost-effective.

Although our data showed the impact of miRNA methylation on PFS, the T classification was an outstandingly strong determiner for PFS. Obtaining a greater number of study subjects and redesigning the study into a comparison within a single T status would be essential to assess the capability of miRNA methylation as a potential biomarker for cancer prognosis.

In summary, we analyzed the CpG island methylation statuses of *mi-152, -9-3, -124-1, -124-2,* and *-124-3* in NSCLC. We found that the methylation of multiple miRNA loci was associated with an advanced T status as well as a poor PFS in a univariate analysis. Our result enlightens the accumulation of aberrant DNA methylation that occurs in concordance with the tumor progression.

Acknowledgments

This work was supported by grants from the Smoking Research Foundation, the Takeda Science Foundation, and the Japan Society for the Promotion of Science, Grants-in-Aid for Scientific Research (KAKENHI) (20659129, 22790749).

Disclosure Statement

Daiya Takai is supported by research grants from the Smoking Research Foundation and the Takeda Science Foundation.

References

1 Jemal A, Siegel R, Xu J, Ward E. Cancer statistics, 2010. *CA Cancer J Clin* 2010; **60**: 277–300.
2 Lewis BP, Burge CB, Bartel DP. Conserved seed pairing, often flanked by adenosines, indicates that thousands of human genes are microRNA targets. *Cell* 2005; **120**: 15–20.
3 Calin GA, Croce CM. MicroRNA signatures in human cancers. *Nat Rev Cancer* 2006; **6**: 857–66.
4 Takamizawa J, Konishi H, Yanagisawa K *et al.* Reduced expression of the let-7 microRNAs in human lung cancers in association with shortened postoperative survival. *Cancer Res* 2004; **64**: 3753–6.
5 Saito M, Schetter AJ, Mollerup S *et al.* The association of microRNA expression with prognosis and progression in early-stage, non-small cell lung adenocarcinoma: a retrospective analysis of three cohorts. *Clin Cancer Res* 2011; **17**: 1875–82.
6 Kunej T, Godnic I, Ferdin J, Horvat S, Dovc P, Calin GA. Epigenetic regulation of microRNAs in cancer: an integrated review of literature. *Mutat Res* 2011. doi: 10.1016/j.mrfmmm.2011.03.008.
7 Kozaki K, Imoto I, Mogi S, Omura K, Inazawa J. Exploration of tumor-suppressive microRNAs silenced by DNA hypermethylation in oral cancer. *Cancer Res* 2008; **68**: 2094–105.
8 Saito Y, Jones PA. Epigenetic activation of tumor suppressor microRNAs in human cancer cells. *Cell Cycle* 2006; **5**: 2220–2.
9 Watanabe K, Emoto N, Hamano E *et al.* Genome structure-based screening identified epigenetically silenced microRNA associated with invasiveness in non-small-cell lung cancer. *Int J Cancer* 2011. doi: 10.1002/ijc.26254.
10 Lujambio A, Ropero S, Ballestar E *et al.* Genetic unmasking of an epigenetically silenced microRNA in human cancer cells. *Cancer Res* 2007; **67**: 1424–9.
11 Lujambio A, Calin GA, Villanueva A *et al.* A microRNA DNA methylation signature for human cancer metastasis. *Proc Natl Acad Sci USA* 2008; **105**: 13556–61.
12 Sobin LH, Wittekind C, eds. *TNM Classification of Malignant Tumours (Uicc International Union Against Cancer)*, 6th edn. New York, NY: Wiley-Liss, 2002.
13 Sambrook J, Russell DW, eds. *Molecular Cloning: A Laboratory Manual*, 3rd edn. New York, NY: Cold Spring Harbor Laboratory Press, 2001.
14 Sano A, Kage H, Sugimoto K *et al.* A second-generation profiling system for quantitative methylation analysis of multiple gene promoters: application to lung cancer. *Oncogene* 2007; **26**: 6518–25.
15 Xiong Z, Laird PW. COBRA: a sensitive and quantitative DNA methylation assay. *Nucleic Acids Res* 1997; **25**: 2532–4.
16 Watanabe K, Emoto N, Sunohara M *et al.* Treatment of PCR products with exonuclease I and heat-labile alkaline phosphatase improves the visibility of combined bisulfite restriction analysis. *Biochem Biophys Res Commun* 2010; **399**: 422–4.
17 Dudziec E, Miah S, Choudhry HM *et al.* Hypermethylation of CpG islands and shores around specific microRNAs and mirtrons is associated with the phenotype and presence of bladder cancer. *Clin Cancer Res* 2011; **17**: 1287–96.
18 Rakyan VK, Down TA, Thorne NP *et al.* An integrated resource for genome-wide identification and analysis of human tissue-specific differentially methylated regions (tDMRs). *Genome Res* 2008; **18**: 1518–29.
19 Bandres E, Agirre X, Bitarte N *et al.* Epigenetic regulation of microRNA expression in colorectal cancer. *Int J Cancer* 2009; **125**: 2737–43.
20 Agirre X, Vilas-Zornoza A, Jimenez-Velasco A *et al.* Epigenetic silencing of the tumor suppressor microRNA Hsa-miR-124a regulates CDK6 expression and confers a poor prognosis in acute lymphoblastic leukemia. *Cancer Res* 2009; **69**: 4443–53.

doi: 10.1111/j.1349-7006.2011.02101.x

21 Furuta M, Kozaki KI, Tanaka S, Arii S, Imoto I, Inazawa J. miR-124 and miR-203 are epigenetically silenced tumor-suppressive microRNAs in hepatocellular carcinoma. *Carcinogenesis* 2010; **31**: 766–76.
22 Brock MV, Hooker CM, Ota-Machida E *et al.* DNA methylation markers and early recurrence in stage I lung cancer. *N Engl J Med* 2008; **358**: 1118–28.
23 Tian L, Suzuki M, Nakajima T *et al.* Clinical significance of aberrant methylation of prostaglandin E receptor 2 (PTGER2) in nonsmall cell lung cancer: association with prognosis, PTGER2 expression, and epidermal growth factor receptor mutation. *Cancer* 2008; **113**: 1396–403.
24 Kim DS, Kim MJ, Lee JY *et al.* Epigenetic inactivation of Homeobox A5 gene in nonsmall cell lung cancer and its relationship with clinicopathological features. *Mol Carcinog* 2009; **48**: 1109–15.
25 Toyota M, Ahuja N, Ohe-Toyota M, Herman JG, Baylin SB, Issa JP. CpG island methylator phenotype in colorectal cancer. *Proc Natl Acad Sci USA* 1999; **96**: 8681–6.
26 Teodoridis JM, Hardie C, Brown R. CpG island methylator phenotype (CIMP) in cancer: causes and implications. *Cancer Lett* 2008; **268**: 177–86.
27 Liu Z, Zhao J, Chen XF *et al.* CpG island methylator phenotype involving tumor suppressor genes located on chromosome 3p in non-small cell lung cancer. *Lung Cancer* 2008; **62**: 15–22.
28 Zhang Y, Wang R, Song H *et al.* Methylation of multiple genes as a candidate biomarker in non-small cell lung cancer. *Cancer Lett* 2011; **303**: 21–8.
29 Kusakabe M, Kutomi T, Watanabe K *et al.* Identification of G0S2 as a gene frequently methylated in squamous lung cancer by combination of in silico and experimental approaches. *Int J Cancer* 2010; **126**: 1895–902.
30 Baylin S, Bestor TH. Altered methylation patterns in cancer cell genomes: cause or consequence? *Cancer Cell* 2002; **1**: 299–305.
31 Kimura M. Recent development of the neutral theory viewed from the Wrightian tradition of theoretical population genetics. *Proc Natl Acad Sci USA* 1991; **88**: 5969–73.

Supporting Information

Additional Supporting Information may be found in the online version of this article:

Fig. S1. Combined bisulfite restriction analysis results of tumor and adjacent normal tissues from the initial eight non-small-cell lung carcinoma cases.

Fig. S2. Unsupervised hierarchical clustering of the combined bisulfite restriction analysis results of 96 samples of resected eight non-small-cell lung carcinoma tissues with five miRNA loci.

Please note: Wiley-Blackwell are not responsible for the content or functionality of any supporting materials supplied by the authors. Any queries (other than missing material) should be directed to the corresponding author for the article.

Journal of Medical Virology 83:1383–1390 (2011)

Human Papillomavirus Infection in Lung and Esophageal Cancers: Analysis of 485 Asian Cases

Akiteru Goto,[1] Chih-Ping Li,[1] Satoshi Ota,[1] Toshiro Niki,[2] Yuji Ohtsuki,[3] Shinichi Kitajima,[4] Suguru Yonezawa,[4] Chihaya Koriyama,[5] Suminori Akiba,[5] Hisataka Uchima,[6] Yueh-Min Lin,[7] Kun-Tu Yeh,[7] Jae-Soo Koh,[8] Chul-Woo Kim,[9] Kun-Yong Kwon,[10] Min En Nga,[11] and Masashi Fukayama[1]*

[1]*Department of Human Pathology, Graduate School of Medicine, The University of Tokyo, Tokyo, Japan*
[2]*Department of Pathology, School of Medicine, Jichi Medical School, Tochigi, Japan*
[3]*Department of Pathology, Kochi Medical School, Kochi, Japan*
[4]*Department of Human Pathology, Field of Oncology, Kagoshima University Graduate School of Medical and Dental Sciences, Kagoshima, Japan*
[5]*Department of Epidemiology and Preventive Medicine, Kagoshima University Graduate School of Medical and Dental Sciences, Kagoshima, Japan*
[6]*Department of Pathology, Urasoe General Hospital, Okinawa, Japan*
[7]*Department of Pathology, Changhua Christian Hospital, Changhua, Taiwan, Republic of China*
[8]*Department of Pathology, Korea Cancer Center Hospital, Seoul, Korea*
[9]*Department of Pathology, Seoul National University Hospital, Seoul, Korea*
[10]*Department of Pathology, Keimyung University Medical Center, Daegu, Korea*
[11]*Department of Pathology, National University of Singapore, Singapore*

The role of human papillomavirus (HPV) in the development of lung and esophageal cancer remains inconclusive, which is in contrast to the established role HPV plays in the development of uterine cervical cancer. One of the reasons for this is the difference among reported HPV infection rates in these cancers. An analysis of 485 lung and esophageal cancers (176 lung squamous cell carcinoma, 128 lung adenocarcinoma, 181 esophageal carcinoma) in eight institutions in Asia (Tokyo, Kochi, Kagoshima, and Okinawa, Japan; Seoul and Daegu, Korea; Changhua, Republic of China (Taiwan); Singapore, Singapore) was carried out in order to clarify infection rates with HPV. Samples were examined in one laboratory of the Department of Pathology, the University of Tokyo, Japan in order to avoid inter-laboratory variation using a combination of polymerase chain reaction and in situ hybridization (ISH). HPV was found in 6.3%, 7%, and 9.4% of patients with lung squamous cell carcinoma, lung adenocarcinoma, and esophageal cancer, respectively. Among the geographic areas surveyed, Kagoshima exhibited a significantly higher prevalence of HPV infection in cases of esophageal carcinoma (24.1%). There was no geographical difference in the infection rates of HPV in lung carcinomas. Subtype-specific ISH was also performed, which identified the high-risk HPV types 16/18 in the majority (75.7%) of the patients with lung and esophageal cancer positive for HPV. ***J. Med. Virol. 83:1383–1390, 2011.*** © 2011 Wiley-Liss, Inc.

KEY WORDS: human papillomavirus (HPV), Asia; geographical distribution; lung cancer; esophageal cancer

INTRODUCTION

The causative role of human papillomavirus (HPV), a double-stranded circular DNA virus, in uterine cervical cancer is well established: HPV is present in nearly all cervical cancer cases and its oncogenic ability has been previously demonstrated [Zur Hausen, 2009]. Among over 100 HPV types, several specific high-risk types (16, 18, 31, 33, 45, 51, 52, 58, etc.) are

Additional supporting information may be found in the online version of this article.

*Correspondence to: Masashi Fukayama, MD, Department of Human Pathology, Graduate School of Medicine, The University of Tokyo, Hongo 7-3-1, Bunkyo-ku, Tokyo 113-0033, Japan.
E-mail: mfukayama-tky@umin.ac.jp

Accepted 9 May 2011
DOI 10.1002/jmv.22150
Published online in Wiley Online Library (wileyonlinelibrary.com).

responsible primarily for cervical carcinogenesis [Zur Hausen, 2002; Narisawa-Saito and Kiyono, 2007].

In addition to cervical cancer, HPV infection has been reported in various genital and non-genital cancers [Gillison and Shah, 2003; Zur Hausen, 2009]. Among such cancers, anal squamous cell carcinoma and oropharyngeal, lung, and esophageal cancer have a relatively high rate of HPV infection [Gillison and Shah, 2003]. The detection rate differs considerably, particularly in esophageal (0–36%) and lung cancer (3.3–79%) [Hirayasu et al., 1996; Syrjänen, 2002; Gillison and Shah, 2003; Chen et al., 2004], and the carcinogenic role of HPV in both of these cancers remains controversial. The detection rate may be affected by ethnicity or the study method. Meta-analysis is one tool used to estimate the distribution of the rate of HPV infection for these cancers in different ethnic populations and in different regions. However, the meta-analysis results do not necessarily eliminate the effects of inconsistency in detection methods or sampling modalities (i.e., fresh frozen tissue, formalin-fixed paraffin-embedded (FFPE) tissue, or cytology specimens). Thus, we performed this large-scale study in which a standardized detection method was employed in various regions and ethnic populations in order to elucidate the extent of HPV involvement in lung or esophageal carcinogenesis.

A total of 485 Asian cases of lung and esophageal carcinoma were examined for evidence of HPV infection. To ensure precise and reliable data and to avoid inter-method and inter-examiner variation, the sample source was limited to FFPE specimens, and detected HPV using a combination of in situ hybridization (ISH) and polymerase chain reaction (PCR) at a single laboratory. The samples were collected from eight major medical institutions in Asia, including regions HPV-endemic for lung cancer: Okinawa, Japan, and Taichung, China.

SUBJECTS AND METHODS

Study Subjects

In total, 485 Asian cases were analyzed for HPV infection, including 304 cases of lung cancer comprising 176 adenocarcinomas, 128 squamous cell carcinomas, and 181 cases of esophageal squamous cell carcinoma. The samples were obtained from eight medical institutions in four Asian countries: Japan (The University of Tokyo Hospital, Tokyo; Kochi University Hospital, Kochi; Kagoshima University Hospital, Kagoshima; and Urazoe General Hospital, Okinawa), Korea (Korean Cancer Center, Seoul, and Keimyung University Hospital, Daegu), Republic of China (Changhua Christian Hospital, Changhua), and Singapore (National Singapore University Hospital). The ethnicity of the case from each country was matched using the name of the patient prior to anonymization for the study. The number of cases obtained from each institute is shown in Table I and demographic profiles of the cases are provided in Table II. Patient history of tobacco-smoking was available for University of Tokyo Hospital cases, in which all patients with lung squamous cell carcinoma and esophageal cancer, as well as 16 out of 22 patients with lung adenocarcinoma, were smokers. Representative 4-μm-thick tumor tissue sections of FFPE specimens were collected for examination. Samples from Singapore National University Hospital were collected in the form of tissue microarray with the core representing 30 lung cancer cases (15 adenocarcinomas and 15 squamous cell carcinomas).

Approval for this study was obtained in accordance with the legal regulations of each country by the appropriate Institutional Review Boards. All samples were obtained at the time of surgery.

HPV Detection by PCR

From each case, DNA was isolated from three sections (with the exception of the tissue microarray samples from Singapore) using a Puregene Tissue Kit (Qiagen, Valencia, CA) according to the manufacturer's instructions. Initially, three 5-μm-thick sections of a FFPE sample from each case were deparaffinized in 1,200 μl of xylene in a 2 ml microcentrifuge tube. Deparaffinized samples were incubated with Proteinase K at 55°C overnight and then with RNAse A at 37°C for 15 min. After removing precipitated proteins formed by the protein precipitation solution, DNA was precipitated and retrieved using isopropanol. All of

TABLE I. Number of Cases From Participating Institutions

		Number of cases		
	Country	Lung squamous cell carcinoma	Lung adenocarcinoma	Esophageal cancer
University of Tokyo Hospital, Tokyo	Japan	22	22	23
Kochi University Hospital, Kochi	Japan	10	10	21
Kagoshima University Hospital, Kagoshima	Japan	25	0	29
Urazoe General Hospital, Okinawa	Japan	5	8	3
Korean Cancer Center, Seoul	Korea	30	10	40
Keimyung University Hospital, Daegu	Korea	34	33	34
Changhua Christian Hospital, Changhua	Republic of China	35	30	31
National Singapore University Hospital, Singapore	Singapore	15	15	0
Total		176	128	181

TABLE II. Demographic Profiles of Lung and Esophageal Cancer Cases

Area	Country	Number of cases	Age in years, mean (SD)	Gender (male:female)	Histological differentiation (w:m:p)
(a) Lung squamous cell carcinoma					
Tokyo	Japan	22	70.1 ± 6.96	20:2	4:8:10
Kochi	Japan	10	65.9 ± 6.23	8:2	2:6:2
Kagoshima	Japan	25	67.8 ± 7.99	24:1	5:12:8
Okinawa	Japan	5	70.4 ± 7.77	3:2	1:4:0
Seoul	Korea	30	62.3 ± 7.62	28:2	5:20:5
Daegu	Korea	34	NA	NA	NA
Changhua	ROC	35	67.0 ± 8.14	34:1	2:27:6
Singapore	Singapore	15	NA	NA	NA
Total		176 (127 cases informative for demographic information)	67.1 ± 10.0	117:10	19:77:31
(b) Lung adenocarcinoma					
Tokyo	Japan	22	65.7 ± 9.71	19:3	10:9:3
Kochi	Japan	10	68.5 ± 9.70	6:4	4:2:4
Kagoshima	Japan	0	NA	NA	NA
Okinawa	Japan	8	72.0 ± 9.05	7:1	2:4:2
Seoul	Korea	10	60.3 ± 7.13	7:3	2:5:3
Daegu	Korea	33	NA	NA	NA
Changhua	ROC	30	68.4 ± 10.77	18:12	15:12:3
Singapore	Singapore	15	NA	NA	NA
Total		128 (80 cases informative for demographic information)	66.6 ± 7.98	57:23	33:32:15
(c) Esophageal cancer					
Tokyo	Japan	23	61.7 ± 8.67	19:4	8:7:8
Kochi	Japan	21	64.2 ± 7.86	20:1	3:13:5
Kagoshima	Japan	29	64.3 ± 11.10	28:1	13:13:3
Okinawa	Japan	3	60.0 ± 8.89	2:1	1:0:2
Seoul	Korea	40	62.1 ± 6.78	38:2	15:23:2
Daegu	Korea	34	NA	NA	NA
Changhua	ROC	31	57.3 ± 10.42	31:0	9:19:3
Singapore	Singapore	0	NA	NA	NA
Total		181 (147 cases informative for demographic information)	62.0 ± 9.24	138:9	49:75:23

w, well differentiated carcinoma; m, moderately differentiated carcinoma; p, poorly differentiated carcinoma; NA, not available; ROC, Republic of China.

the reagents, aside from xylene, were obtained through the manufacturer. DNA yields were measured by absorbance at 260 nm (A260), and DNA purity was determined using the ratio of absorbance at 260 nm to absorbance at 280 nm (A260/A280). Scans were performed using a Beckman spectrophotometer DU 730 (Beckman Coulter Inc., Brea, CA). The DNA yields averaged 21.4 μg/ml per sample, with a minimum 5.46 μg/ml and maximum 66.24 μg/ml. DNA purity (A260/A280) averaged 1.98 with a standard deviation of 0.39. There was no significant difference in DNA yield or DNA purity between the samples of various institutions or between cancer types. *Beta-globin* PCR was performed to confirm the quality and quantity of DNA extracted for HPV detection. The 110 base pair *beta-globin* gene PCR product was detected in all DNA samples in accordance with the method of Saiki et al. [1985]. For HPV detection, GP5+ and GP6+ primers (GP5+: 5′-TTTGTTACTGTGGTAGATACTAC-3′ and GP6+: 3′-CTTATACTAAATGTCAAATAAAAAG-5′) were employed; these primers were designed to detect highly conserved HPV genome sequences [Yoshikawa et al., 1991]. In a preliminary study, we found that PCR using GP5+/6+ primers detected 1–10 copies of HPV in DNA extracted from Hela cells with a known HPV infection.

PCR was performed on 0.1 μg of extracted DNA using G5+ and G6+ primers (50 pmol each), 5 units of Taq DNA polymerase (Takara, Tokyo, Japan), 200 μM dNTP, 3.5 mM $MgCl_2$ in 50 mM KCl, and 10 mM Tris–HCl (pH 8.3). The standard DNA amplification conditions employed were as follows: denaturation for 4 min at 94°C, 40 cycles with denaturation for 1 min at 94°C, 2 min of annealing at 40°C, and 1.5 min of extension at 72°C. The final extension step at 72°C was increased to 4 min. PCR products were electrophoresed on agarose gels (3% Nusieve GTC; FMC Bioproducts, Rockland, ME) and photographed.

In Situ Hybridization for HPV

For the initial screening, we performed ISH using a wide-spectrum HPV probe on all cases. Subtype-specific HPV-ISH and/or PCR was then performed for the cases that tested positive in the screening.

The ISH screening was performed using a biotinylated wide-spectrum HPV probe cocktail detecting DNA–HPV types 6, 11, 16, 18, 31, 33, 35, 45, 51, and 52 (Y1443; Dako Japan, Tokyo, Japan). Additional typing of HPV was performed using biotinylated HPV probe cocktails for types 6/11 (Y1411; Dako) and for types 16/18 (Y1412; Dako). Sections were deparaffinized, digested with Proteinase K (0.25 mg/ml for 10 min at 37°C), and rehydrated. Background quenching for 20 min was performed using 0.3% hydrogen peroxide in methanol. Target and probe DNA samples were denatured at 95°C for 5 min, and hybridization was performed in a 5% CO_2 humidified chamber overnight at 37°C. Following stringent wash, GenPoint Tyramide Signal Amplification System (K0620; Dako Japan) was used according to the manufacturer's instructions. First, sections were incubated in a 1:100 dilution of primary streptavidin-HRP for 15 min, washed, and then incubated with a biotinyl tyramide solution for 15 min at room temperature. This was followed by incubation with secondary streptavidin-HRP for 15 min and diaminobenzidine chromogen for 5 min. Sections were counterstained with hematoxylin, dehydrated, and mounted. Negative controls (with the omission of probes) and positive controls (sections of SiHa cells with HPV 16 infection [K0629; Dako] and uterine low-grade squamous intraepithelial lesions with HPV 11 infection) were included for each test. Using light microscopy, ISH results were evaluated independently by two researchers (AG and CL). Cases with HPV signals in the nuclei of tumor cells were determined to be positive.

Statistical Methods

Chi-square and Fisher's exact tests were performed using the Statview computer program (Abacus Concepts, Berkeley, CA). The results were considered to be significant if the P-value was < 0.05.

RESULTS

The HPV signals in the HPV-ISH-positive cases observed in the nuclei of the tumor cells demonstrated an integrated form of HPV DNA [Cooper et al., 1991] (Fig. 1).

Demographic profiles of the cases exhibiting HPV infection are shown in Table III. In total, 37 lung and esophageal cancers out of 485 cases (7.6%) were determined to be positive for HPV by PCR and/or wide-spectrum ISH.

Geographical Distribution of HPV Infection in Lung and Esophageal Cancers

HPV detection rates, subdivided by cancer type and geographic region, are illustrated in Figure 2. The data is also provided in Supplementary Table I.

Notably, the highest detection rate was observed in esophageal cancer from Kagoshima, Japan (7/29 cases, 24.1%); this was a significantly higher detection rate compared to esophageal cancer cases from Tokyo, Kochi, or Seoul ($P < 0.05$). Moreover, in Kagoshima the HPV infection rate for esophageal cancer was significantly higher than that of lung squamous cell carcinoma.

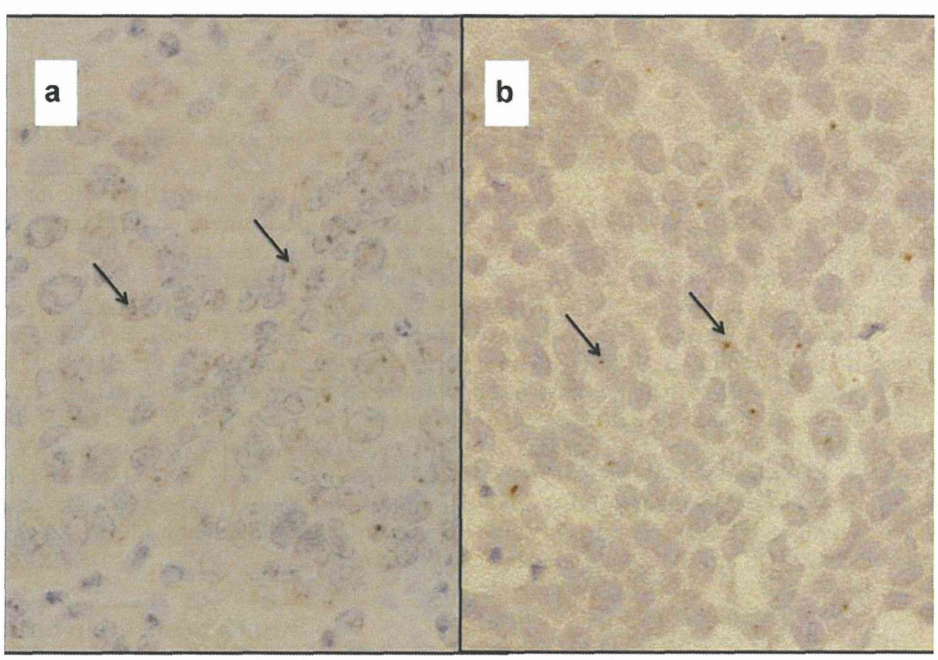

Fig. 1. Representative case of HPV-positive esophageal carcinoma. ISH, using wide-spectrum HPV probe cocktail, showed dot-like signals in nuclei of cancer cells (arrow), which suggests integration of HPV into host genome. [Color figure can be viewed in the online issue, which is available at wileyonlinelibrary.com]

TABLE III. Characteristics of the Lung and Esophageal Cancer Cases With HPV Infection

	Area	Country	PCR	Wide-spectrum ISH	Subtype-specific ISH		Age	Gender	Histological differentiation
					HPV 6/11	HPV 16/18			
(a) Lung squamous cell carcinoma									
1	Tokyo	Japan	−	+	+	−	72	Male	m
2	Kochi	Japan	+	−	−	+	69	Male	m
3	Kagoshima	Japan	+	−	−	−	74	Male	m
4	Okinawa	Japan	+	+	+	+	59	Male	m
5	Seoul	Korea	−	+	+	−	60	Male	w
6	Daegu	Korea	−	+	+	+	NA	NA	NA
7	Daegu	Korea	+	+	−	+	NA	NA	NA
8	Daegu	Korea	+	−	+	+	NA	NA	NA
9	Changhua	ROC	+	+	−	+	61	Male	m
10	Changhua	ROC	+	+	+	+	63	Male	m
11	Changhua	ROC	+	+	+	+	72	Male	m
(b) Lung adenocarcinoma									
1	Kochi	Japan	+	−	−	+	46	Female	w
2	Okinawa	Japan	+	+	−	+	75	Male	w
3	Seoul	Korea	+	+	+	+	64	Male	p
4	Seoul	Korea	+	−	−	+	46	Female	m
5	Daegu	Korea	−	+	−	−	NA	NA	NA
6	Changhua	ROC	+	−	−	+	55	Male	w
7	Changhua	ROC	−	+	+	+	79	Male	w
8	Changhua	ROC	+	+	−	−	65	Male	m
9	Changhua	ROC	+	−	+	+	71	Male	p
(c)Esophageal carcinoma									
1	Tokyo	Japan	−	+	+	+	53	Male	w
2	Kagoshima	Japan	−	+	+	−	68	Male	w
3	Kagoshima	Japan	−	+	−	+	64	Male	m
4	Kagoshima	Japan	+	+	+	+	70	Male	m
5	Kagoshima	Japan	+	+	+	+	72	Male	w
6	Kagoshima	Japan	−	+	−	+	86	Male	m
7	Kagoshima	Japan	+	+	+	+	65	Male	w
8	Kagoshima	Japan	+	+	+	−	52	Male	m
9	Seoul	Korea	+	−	−	+	67	Male	w
10	Seoul	Korea	+	+	+	−	60	Male	m
11	Seoul	Korea	+	+	+	−	60	Male	m
12	Seoul	Korea	−	+	+	+	59	Male	w
13	Daegu	Korea	−	+	−	+	NA	NA	NA
14	Daegu	Korea	−	+	+	+	NA	NA	NA
15	Daegu	Korea	+	−	+	+	NA	NA	NA
16	Changhua	ROC	−	+	−	+	43	Male	m
17	Changhua	ROC	+	+	+	+	47	Male	m

(+), positive; (−), negative; m, moderately differentiated cancer; w, well-differentiated cancer; NA, not available; age, age in years; ROC, Republic of China.

For lung cancers, there was no significant difference in the HPV detection rate between regions or countries. Additionally, there was no correlation between the HPV detection rate of lung and esophageal cancers within a region (data not shown).

Clinicopathological Characteristics of Cases With HPV Infection

The clinicopathological information for each case in six of eight participating institutions, including age, gender, and histological differentiation of the tumor, is shown in Table II. For HPV-positive cases, the factors are summarized in Tables III and IV. HPV-positive lung and esophageal cancer cases did not significantly differ from HPV-negative cases for these clinicopathological factors. Tobacco-smoking history was available for the cases from Tokyo in which all HPV-positive lung squamous cell carcinoma and esophageal cancer cases involved smokers.

HPV types in Lung and Esophageal Cancers

In cases that tested positive for HPV by PCR and/or wide-spectrum ISH, type-specific ISH was performed; results are shown in Figure 3.

The majority of the cases (28/37 cases, 75.7%) were positive for HPV 16/18 ISH—the high-risk types of HPV. Among these cases, 15 cases showed dual positivity for HPV 6/11 and HPV 16/18 ISH. Notably, there was dual positivity in esophageal cancer in 8/17 cases (47.1%).

Comparison of HPV Detection Results Between PCR and ISH

Two methods were employed in screening the 455 cases in this study: PCR using HPV common primers

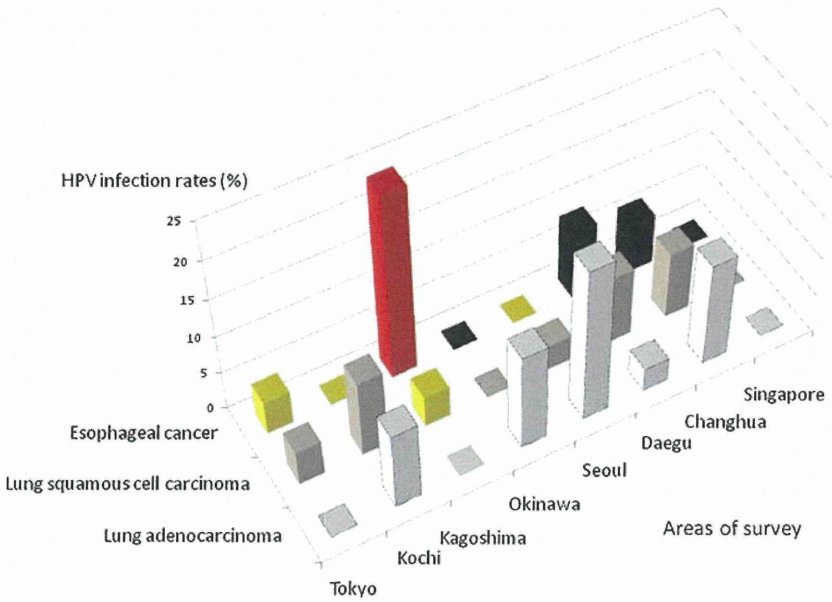

Fig. 2. HPV infection rates in lung and esophageal cancers by areas in Asia. The height of the bars illustrates HPV infection rate (%) for lung adenocarcinoma, lung squamous cell carcinoma, and esophageal carcinoma in each area. HPV infection rate for esophageal carcinoma in Kagoshima, Japan (24.1%, red-colored) was significantly higher than groups shown with yellow-colored bars (esophageal cancer in Tokyo, Kochi, Daegu, and lung squamous cell carcinoma in Kagoshima).

GP5+/GP6+, and ISH using a wide-spectrum HPV probe cocktail. The comparison of PCR results with those of ISH is shown in Table V. The results of PCR and wide-spectrum ISH were significantly correlated ($P < 0.0001$). The results obtained in terms of sensitivity and specificity when using the HPV positive screening method of PCR with GP5+/GP6+ were 57.7% and 97.9%, respectively, whereas the results obtained when using PCR along with wide-spectrum ISH were 76.4% and 98.1%, respectively.

DISCUSSION

In the present study concerning HPV detection in lung and esophageal cancers, a multi-institutional study of Asian populations, inclusive of HPV-endemic areas, was conducted. Okinawa, one of the southwestern islands of Japan, is notable for its relatively high incidence of HPV infection in cases of lung squamous cell carcinoma—79% of cases have previously been reported to be positive for HPV [Hirayasu et al., 1996; Miyagi et al., 2000]. In the present study, the rate (20%) was relatively lower than that reported in 1993. Miyagi et al. [2000] also analyzed another cohort that demonstrated 68%, 35%, 23%, and 24% infection rates in 1995, 1996, 1997, and 1998, respectively. This indicated a downward trend of the HPV infection rate for lung squamous cell carcinoma in Okinawa, a finding supported by the results of the present study in which samples obtained in 1999 and 2000 were analyzed. Miyagi et al. [2000] further attributed the decline of the overall HPV infection rate to a change in the distribution of histologically differentiated carcinomas in Okinawa: well-differentiated carcinoma with a high rate of HPV infection to moderately or poorly differentiated carcinoma with a low rate of infection.

Kagoshima in Japan was identified as the region exhibiting the highest rate of HPV (24.1%) in cases of esophageal cancer. This may be attributable to geographic variation rather than ethnicity, as other parts of Japan (areas such as Tokyo and Kochi) did not reveal a similarly high infection rate for HPV in

TABLE IV. Clinicopathological Characteristics of Lung and Esophageal Cancer Cases With and Without HPV Infection

	Age in years (mean)	Gender (male:female)	Histological differentiation (w:m:p)
Lung squamous cell carcinoma	**66.3**/67.2	**8:0**/109:10	**1:7:0**/18:70:31
Lung adenocarcinoma	**62.6**/63.2	**6:2**/51:21	**4:2:2**/29:30:15
Esophageal cancer	**61.9**/62.5	**14:0**/124:9	**6:7:0**/43:68:23

HPV-positive case (bold)/HPV-negative case.
w, well-differentiated carcinoma; m, moderately differentiated carcinoma; p, poorly differentiated carcinoma.

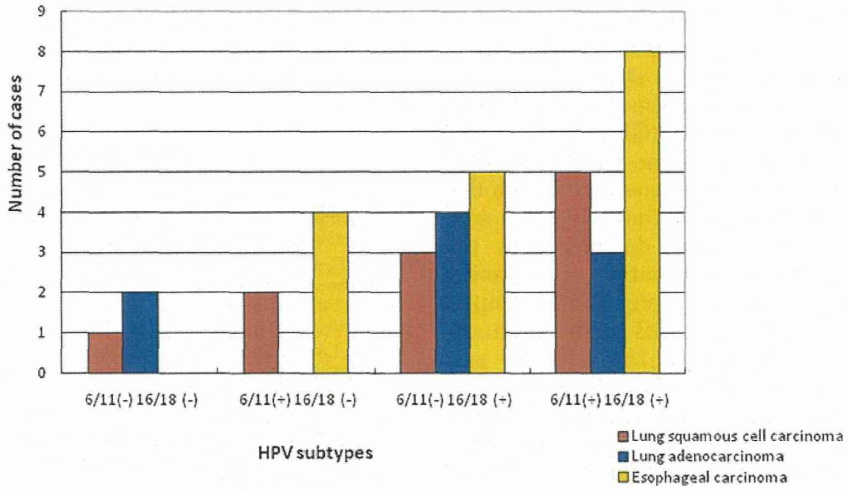

Fig. 3. HPV subtypes in lung and esophageal carcinomas. The subgroups were categorized by HPV 6/11 and HPV 16/18 infection status. Most of the cases (28/37 cases, 75.7%) were positive for HPV 16/18 ISH—the high-risk subtypes of HPV. Co-infection of HPV 6/11 and HPV 16/18 was observed in 15 cases (15/37 cases, 40.5%). [Color figure can be viewed in the online issue, which is available at wileyonlinelibrary.com]

esophageal cancer. Kagoshima is located at the southern end of Kyushyu Island, Japan. Fukuoka, in the northern part of Kyusyu Island, has also been reported to exhibit a relatively high rate of HPV infection (22.6%) in cases of esophageal carcinoma [Kawaguchi et al., 2000]. In contrast, reports from Honshu Island, the Japanese mainland, indicated a lack of HPV prevalence in squamous cell carcinomas [Mizobuchi et al., 1997]. Kyushyu Island may therefore be considered an HPV-endemic region for esophageal cancers. Such intra-national variance, between 0% and 44%, has also been observed in India [Shukla et al., 2009]. The results of the present study are in concordance with this finding when the HPV infection rate of 5% in lung cancer in India is taken into consideration, which is comparable to our data in Asian countries [Shukla et al., 2009].

Lung and esophageal carcinomas are both thoracic cancers with similar etiological factors (tobacco smoking) and demography (male predominance and greater age at diagnoses) [Hirayasu et al., 1996; Syrjänen, 2002]. Despite these similarities, HPV infection for these cancers has not been correlated previously with the regions surveyed. Several recent lines of evidence suggest that additional genetic factors of the host, such as mutation of *ras* and *myc* amplification, are required for the development of cervical cancer, in addition to the deregulated expression of HPV oncogenes [Narisawa-Saito et al., 2008]. Such genetic factors may modify HPV-related carcinogenesis in lung and esophageal cancers, which would explain the variability between the infection rates of these cancers. Additionally, tobacco-smoking status may also influence HPV infection rates [Cheng et al., 2001]. Information on tobacco smoking was limited for the present study, however, and further epidemiological investigation is warranted to clarify the relationship between HPV infection of these cancers and tobacco smoking or genetic abnormalities.

TABLE V. Comparison of HPV Detection Results Between PCR and Wide-Spectrum ISH

	HPV-wide spectrum ISH	
	(+)	(−)
HPV-PCR (+)	15	9
HPV-PCR (−)	11	420
	Number of cases	$P < 0.0001$

(+), positive; (−), negative.

In the present study, 16 out of 28 high-risk HPV16/18-positive cases were also positive for HPV 6/11 and low-risk types of HPV 6/11, such as laryngeal papillomas and respiratory papillomatosis [Gillison and Shah, 2003], which are associated predominantly with the upper aerodigestive respiratory tract. Co-infection of these high- and low-risk HPV types was also noted in lung squamous cell carcinoma and a superimposition of low-risk types of HPV infection in HPV16/18-positive cancers has been suggested [Hirayasu et al., 1996]. In this study, the co-infection rate of 16/28 (57.0%) is high, considering the HPV infection rate of 8.1% in the total study cases. Vulnerability in immune surveillance may exist for HPV in such cases of co-infection of HPV subtypes. The ISH-based typing utilized in this study did not distinguish HPV 16 and HPV18 infection in the cases. HPV18 is reportedly predominate in lung cancers, whereas HPV16 is predominate in esophageal cancer [Shukla et al., 2009]; this predominance may well apply to the cohort of the present study.

In epidemiological studies, multiple methods have been used previously to detect HPV. These include

Southern blot, PCR, and ISH. Therefore, inter-method variations have potentially affected the variations in previously reported results. In this study, the results correlated in a high percentage of the samples (95.6%) by PCR using common primers (GP5+/GP6+) and wide-spectrum ISH. However, some cases exhibited discrepancies in the results. In 20 cases with such discrepancies, 18 cases were positive for HPV upon subtype-specific ISH analysis. This demonstrates the importance of employing a combination of screening methods, particularly in studies using FFPE samples in which the results of PCR and ISH might fluctuate. The sensitivity of wide-spectrum ISH (76.4%) surpassed that of PCR (57.7%) in the present study. It is notable that only three out of seven (42.9%) ISH-positive cases were positive by PCR in samples from Daegu, Korea, whereas seven out of nine (77.8%) ISH-positive cases were positive in samples from Changhua, Taiwan (Table III). Differences in FFPE sample processing or storage status among institutions may have resulted in such inter-institutional variance in PCR sensitivity, and ISH may be a more robust method to evaluate HPV infection from multiple institutions. Recently, several methods, including HC2 assay, INNO-LiPA, and HPV Chip have been developed to detect HPV with high specificity and sensitivity, and the utilization of these methods may improve the quality of molecular epidemiological studies using archived FFPE cancer samples [Bharti et al., 2010]. However, these methods have been basically created to detect HPV infection in non-FFPE uterine cervical specimens; thus, validation studies may be required to detect HPV in archived FFPE samples using these methods.

The present large-scale study investigated the rate of HPV in esophageal carcinoma in Asia, where the major histological type of esophageal cancer is squamous cell carcinoma. In contrast, the major histological type of esophageal cancer in western countries is adenocarcinoma, in which the majority of cases develop in Barrett's esophagus and commonly remain in a precancerous state. HPV has been reportedly identified in 31% of esophageal adenocarcinoma cases in the North American population [Iyer et al., 2010]. The higher HPV infection rate of esophageal cancer in North America compared to the present results could be attributable to the difference in the histological type rather than the regional difference. Even with an adjustment for cancer histology in the present study, the difference in HPV infection rates between regions might be due to another confounding factor.

In conclusion, 485 tumors in Asia were analyzed and 6.3%, 7.0%, and 9.4% of cases tested positive for HPV in lung squamous cell carcinoma, lung adenocarcinoma, and esophageal cancer, respectively. This study demonstrated that the presence of HPV infection in these cancers occurs at a relatively low rate in Asia.

REFERENCES

Bharti AC, Shukla S, Mahata S, Hedau S, Das BC. 2010. Human papillomavirus and control of cervical cancer in India. Expert Rev Obstet Gynecol 5:329–346.

Chen YC, Chen JH, Richard K, Chen PY, Christiani DC. 2004. Lung adenocarcinoma and human papillomavirus infection. Cancer 101:1428–1436.

Cheng YW, Chiou HL, Sheu GT, Hsieh LL, Chen JT, Chen CY, Su JM, Lee H. 2001. The association of human papillomavirus 16/18 infection with lung cancer among non-smoking Taiwanese women. Cancer Res 61:2799–2803.

Cooper K, Herrington CS, Stickland JE, Evans MF, McGee JO. 1991. Episomal and integrated human papillomavirus in cervical neoplasia shown by non-isotopic in situ hybridisation. J Clin Pathol 44:990–996.

Gillison ML, Shah KV. 2003. Chapter 9: Role of mucosal human papillomavirus in nongenital cancers. J Natl Cancer Inst Monogr 31:57–65.

Hirayasu T, Iwamasa T, Kamada Y, Koyanagi Y, Usuda H, Genka K. 1996. Human papillomavirus DNA in squamous cell carcinoma of the lung. J Clin Pathol 49:810–817.

Iyer A, Rajendran V, Adamson CS, Peng Z, Cooper K, Evans MF. 2010. Human papillomavirus is detectable in Barrett's esophagus and esophageal carcinoma but is unlikely to be of any etiologic significance. J Clin Virol 50:205–208.

Kawaguchi H, Ohno S, Araki K, Miyazaki M, Saeki H, Watanabe M, Tanaka S, Sugimachi K. 2000. p53 polymorphism in human papillomavirus-associated esophageal cancer. Cancer Res 60:2753–2755.

Miyagi J, Tsuhako K, Kinjo T, Iwamasa T, Hirayasu T. 2000. Recent striking changes in histological differentiation and rate of human papillomavirus infection in squamous cell carcinoma of the lung in Okinawa, a subtropical island in southern Japan. J Clin Pathol 53:676–684.

Mizobuchi S, Sakamoto H, Tachimori Y, Kato H, Watanabe H, Terada M. 1997. Absence of human papillomavirus-16 and -18 DNA and Epstein–Barr virus DNA in esophageal squamous cell carcinoma. Jpn J Clin Oncol 27:1–5.

Narisawa-Saito M, Kiyono T. 2007. Basic mechanisms of high-risk human papillomavirus-induced carcinogenesis: Roles of E6 and E7 proteins. Cancer Sci 98:1505–1511.

Narisawa-Saito M, Yoshimatsu Y, Ohno S, Yugawa T, Egawa N, Fujita M, Hirohashi S, Kiyono T. 2008. An in vitro multistep carcinogenesis model for human cervical cancer. Cancer Res 68: 5699–5705.

Saiki RK, Scharf S, Faloona F, Mullis KB, Horn GT, Erlich HA, Arnheim N. 1985. Enzymatic amplification of beta-globin genomic sequences and restriction site analysis for diagnosis of sickle cell anemia. Science 230:1350–1354.

Shukla S, Bharti AC, Mahata S, Hussain S, Kumar R, Hedau S, Das BC. 2009. Infection of human papillomaviruses in cancers of different human organ sites. Indian J Med Res 130:222–233.

Syrjänen KJ. HPV infections and oesophageal cancer. J Clin Pathol 2002. 55:721–728.

Yoshikawa H, Kawana T, Kitagawa K, Mizuno M, Yoshikura H, Iwamoto A. 1991. Detection and typing of multiple genital human papillomaviruses by DNA amplification with consensus primers. Jpn J Cancer Res 82:524–531.

Zur Hausen H. 2002. Papillomaviruses and cancer: From basic studies to clinical application. Nat Rev Cancer 2:342–350.

Zur Hausen H. 2009. Papillomaviruses in the causation of human cancers – A brief historical account. Virology 384:260–265.

Pathology International

Pathology International 2011; **61**: 319–321 doi:10.1111/j.1440-1827.2011.02654.x

Case Report

Multicystic mesothelioma of the pericardium

Shigeki Morita,[1] Akiteru Goto,[1] Takashi Sakatani,[1] Satoshi Ota,[1] Tomohiro Murakawa,[2] Jun Nakajima,[2] Eriko Maeda[3] and Masashi Fukayama[1]

[1]*Department of Human Pathology, Graduate School of Medicine, The University of Tokyo, Departments of* [2]*Cardiothoracic Surgery and* [3]*Radiology, The University of Tokyo Graduate School of Medicine, Tokyo, Japan*

Multicystic mesothelioma is a well recognized but rare serosal tumor which mainly arises from the peritoneum in women and is considered as a benign lesion. This is the second case report of pericardial multicystic mesothelioma, which took a fatal clinical course. A 63-year-old man presented with pitting edema, shortness of breath, and hoarseness. Radiological investigations revealed solid and cystic tumor of the pericardium which was continuously extending into the mediastinum and the liver. Pericardial biopsy showed micro-cystic tumor lined by single layer of mesothelial cells without atypia, and the diagnosis was multicystic mesothelioma. Curative surgery could not be performed, and three years and four months later, the patient died because of the direct compression of the heart by the tumor. At autopsy, the tumor was found to be directly extending into the right pleural cavity and the right lung, besides the mediastinum and the liver. Neither malignant transformation nor metastatic tumor was identified.

Key words: autopsy, mesothelioma, multicystic mesothelioma, pericardium, postmortem CT

INTRODUCTION

Multicystic mesothelioma mainly arises from the peritoneal surfaces of young to middle-aged women.[1–5] The tumor is considered as neoplastic lesion by some authors and as hyperplastic reactive lesion by others, and its prognosis is generally accepted as favorable. Multicystic mesothelioma arising in the pericardium is exceedingly rare, and only one infantile case with Down's syndrome has been documented so far.[6] We herein report an adult case of pericardial multicystic mesothelioma with fatal clinical course.

Correspondence: Masashi Fukayama, MD, Department of Pathology, Graduate School of Medicine, The University of Tokyo, Hongo 7-3-1, Bunkyo-ku, Tokyo 113-0033, Japan. Email: mfukayama-tky@umin.net

Received 16 November 2010. Accepted for publication 23 December 2010.

CLINICAL SUMMARY

A 62-year-old man without history of asbestos inhalation was admitted to a nearby hospital complaining of pitting edema and the needle biopsy was not diagnostic. Two years later, he was admitted to The University of Tokyo Hospital complaining of shortness of breath, and hoarseness. As the lesion was diffusely occupying the pericardial cavity, and was strongly adhesive to surrounding structures, curative resection of the tumor could not be performed. His condition deteriorated due to direct compression of the heart by the lesion and pneumonia, although the status of the tumor was stable after the chemotherapy with gemcitabin. He died three years and four months after the first admission to our hospital. At that time, his plasma brain natriuretic peptide level (BNP) was 153.8 pg/mL (normal level: ≤18.4 pg/mL), while BNP level one month before his death was 538.1 pg/mL.

PATHOLOGICAL AND RADIOLOGICAL FINDINGS

Computed tomography (CT) images on admission revealed solid and cystic tumor diffusely surrounding the heart and expanding into the upper mediastinum and the liver along the falciform ligament. The solid component was 1–2 cm thick, and showed intense enhancement suggestive of hypervascularity. Just below the ventricular apex, there was a large solid component of about 3x8 cm, and this component was associated with a nonenhancing core with calcification. Radiologically, this pericardial component was considered to be the primary lesion. The cystic component was 1–6 cm in diameter, and distributed throughout the pericardium and the mediastinum (Fig. 1a). Pericardial biopsy disclosed micro-cystic tumor lined by single layer of flattened or cuboidal

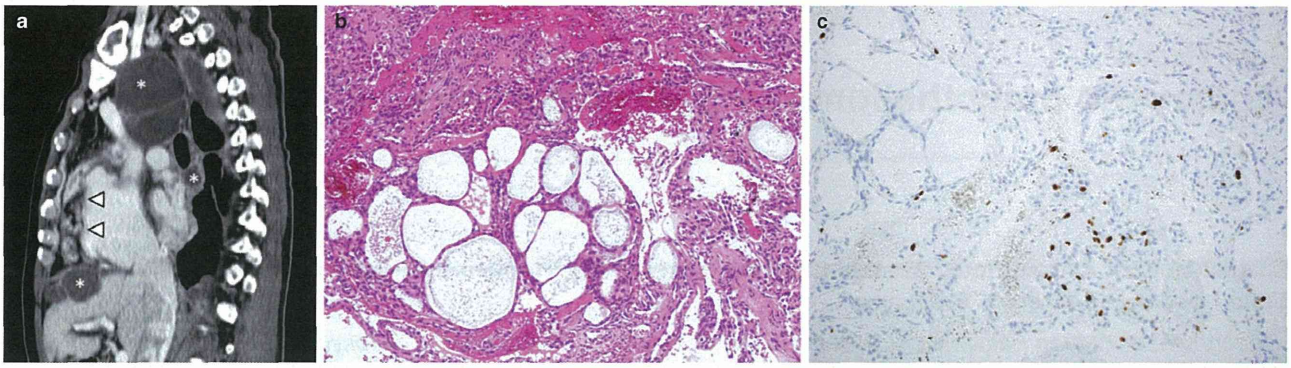

Figure 1 (**a**) Sagittal reconstruction section of contrast-enhanced computed tomography (CT) on admission. Multiple cystic masses are observed in the upper mediastinum and the liver with fluid density contents (asterisk). The pericardial tumor behind the ribs shows irregular enhancement effect (arrow head). (**b**) Histological appearance of the pericardial biopsy specimen. The micro-cystic lesions are lined by single layer of flattened or cuboidal mesothelial cells without atypia. (**c**) MIB-1 labeling index is less than 5% at biopsy.

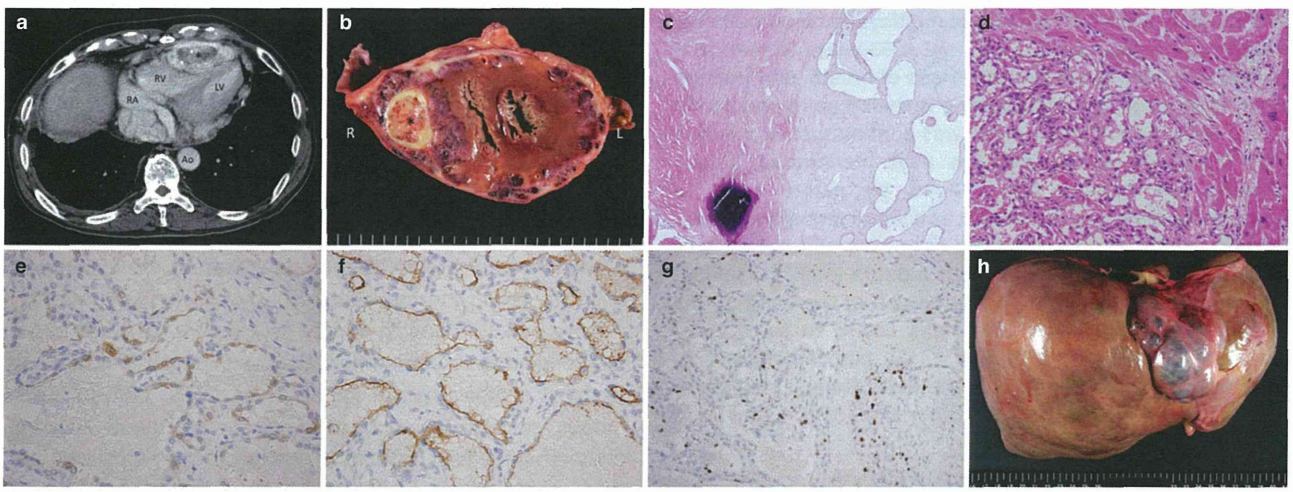

Figure 2 (**a**) Axial contrast-enhanced computed tomography (CT) on admission shows the hypoattenuating lesion with tiny calcifications in the hyperattenuating mass around the heart (asterisk). LV, Left ventricle; RA, Right Atrium; RV, Right Ventricle; Ao, Aorta. (**b**) Gross appearance of the tumor surrounding the heart. The grayish white tumor with numerous tiny cysts containing blood has completely obliterated the pericardial space. Hard yellowish white nodule (asterisk) is observed in the pericardium. (**c**) Histological findings of the yellowish white nodule of the pericardium. Several micro-cystic lesions lined by a single layer of mesothelial cells without atypia is observed in a densely hyalinized stroma with a coarse calcification (lower left). (**d**) Histological findings of the heart at the autopsy. The tumor is infiltrating into the myocardium and showing the same histological features as biopsy specimen (Fig. 1b). (**e**) Calretinin staining at autopsy. Focal positivity for calretinin is observed. (**f**) D2-40 staining at autopsy. Diffuse immunostaining for D2-40 is observed. (**g**) MIB-1 labeling index at autopsy. Index at autopsy is 5% or less as well as in biopsy. (**h**) Gross appearance of the liver. Large cystic lesions up to 10 cm in diameter were extending along the falciform ligament.

mesothelial-like cells without significant atypia (Fig. 1b). Those cells were immunohistochemically focal positive for calretinin and D2-40, while they were negative for thyroid transcription factor-1 (TTF-1) and carcinoembryonic antigen (CEA). Also, the cells were positive for epithelial membrane antigen (EMA) and negative for desmin. No abnormal accumulation of p53 was observed, and Ki-67 labeling index was 5 to 6% (Fig. 1c). The pathological findings were consistent with multicystic mesothelioma.

In the postmortem CT images, the tumor infiltration was confirmed in the entire mediastinum, pericardial cavity, the right thoracic cavity, the right lung, and the liver. At autopsy, the tumor showed micro-cystic and slit appearance besides grossly-visible cysts, and a pericardial hyalinizing lesion with calcification which correlates to the CT finding on admission (Fig. 2a–c). The tumor degeneration with hyalinization and calcification was confined to the pericardium, indicating the pericardial origin of the tumor. Tumor extension into the myocardium was also observed (Fig. 2d). Immunohistochemical findings of the tumor, including calretinin, D2-40, and Ki-67, were identical to those of pericardial biopsy (Fig. 2e–g). Although we investigated the whole cardiac wall microscopi-

cally, no malignant transformation was identified at autopsy. The tumor infiltration was identified in liver, right lung, and nearby lymph nodes, which were considered as direct extension rather than metastases (Fig. 2h). No asbestos body was found with iron staining in the lungs, pleura, peritoneum and other organs. The final diagnosis was pericardial multicystic mesothelioma extending into the heart, the mediastinum, the right pleural cavity, the right lung, and the liver.

DISCUSSION

Since the first description by Mennemayar in 1979,[5] approximately 130 cases of multicystic mesothelioma have been documented to date.[1] Multicystic mesothelioma usually is localized to the pelvic peritoneal surface with female predominance.[1,2] To date, only one case of pericardial multicystic mesothelioma has been reported in a 7-year-old boy with Down's syndrome.[6] Thus, female predominance is not clear in pericardial multicystic mesothelioma, and at the same time, specific genetic predisposition, such as Down's syndrome, is not obvious for the development of the disease.

Differential diagnosis of multicystic mesothelioma includes lymphangioma, mesothelioma of the atrioventricular node, adenomatoid tumor, and malignant mesothelioma. In lymphangioma, lymphoid aggregates and smooth muscle bundles in the wall are frequently seen, and lymphangioma is negative for cytokeratin and calretinin. Most patients of the mesothelioma of the atrioventricular node have a history of congenital heart block, while the present case did not have such a symptom and the tumor was not supposed to have developed in the atrial septum.[7] Adenomatoid tumor is usually localized and circumscribed grossly. Epithelial malignant mesothelioma may show multicystic features and bland cytological appearance. However, the prognosis of pericardial malignant mesothelioma is extremely ominous, with a median survival time of less than 6 months.[8,9] Also, abnormal accumulation of p53 and Ki-67 labeling index of higher than 40% are frequently observed in malignant mesothelioma.[10,11] The present case of multicystic mesothelioma was differentiated from other tumors by points described above.

Biological behavior of multicystic mesothelioma has been considered as benign, and the term 'benign multicystic mesothelioma' was proposed.[1] In spite of such general understanding, recurrence or malignant transformation has been reported in multicystic mesothelioma.[2–4,12] Sawh reported that five cases had recurred in a series of 17 cases of the multicystic mesothelioma of the peritoneum.[3] Even though the term is often used to emphasize the difference from diffuse mesothelioma, it would be safe to avoid the usage of the term 'benign multicystic mesothelioma' in the present situation where clinically benign behavior of the tumor is not guaranteed. That is especially the case for multicystic mesothelioma arising in the thorax, as complete resection of tumor is sometimes difficult and the prognostic data is not sufficiently accumulated due to the extremely small number of the cases. It would be reasonable to take multicystic mesothelioma as a lesion of intermediate malignancy between adenomatoid tumor and diffuse mesothelioma as Weiss advocated.[2] The notion is also supported by 5 to 6% of Ki-67 labeling index of the present case, which was between less than 2.7% of adenomatoid tumor and more than 40% of diffuse mesothelioma.[13]

In summary, we report an adult case of pericardial multicystic mesothelioma which took a fatal clinical course because it could not be surgically resected, and it showed extensive growth in the pericardium, mediastinum and right pleural cavity.

REFERENCES

1 Churg A, Cagle PT, Roggli VL, American Registry of P, Armed Forces Institute of P. *Tumors of the serosal membranes: American Registry of Pathology in collaboration with the Armed Forces Institute of Pathology* 2006.

2 Weiss SW, Tavassoli FA. Multicystic mesothelioma: An analysis of pathologic findings and biologic behavior in 37 cases. *Am J Surg Pathol* 1988; **12**: 737–46.

3 Sawh RN, Malpica A, Deavers MT, Jinsong LIU, Silva EG. Benign cystic mesothelioma of the peritoneum: A clinicopathologic study of 17 cases and immunohistochemical analysis of estrogen and progesterone receptor status. *Human Pathol* 2003; **34**: 369–74.

4 Ross MJ, Welch WR, Scully RE. Multilocular peritoneal inclusion cysts (so-called cystic mesotheliomas). *Cancer* 1989; **64**: 1336–46.

5 Mennemeyer R, Smith M. Multicystic, peritoneal mesothelioma. A report with electron microscopy of a case mimicking intra-abdominal cystic hygroma (Lymphangioma). *Cancer* 1979; **44**: 692–98.

6 Drut Q. Multilocular mesothelial inclusion cysts (so-called benign multicystic mesothelioma) of pericardium. *Histopathology* 1999; **34**: 472–74.

7 Balasundaram S, Halees S, Duran C. Mesothelioma of the atrioventricular node: First successful follow-up after excision. *Eur Heart J* 1992; **13**: 718–9.

8 Thomason R, Schlegel W, Lucca M, Cummings S, Lee S. Primary malignant mesothelioma of the pericardium. Case report and literature review. *Tex Heart Inst J* 1994; **21**: 170–4.

9 Eren NT, Akar AR. Primary pericardial mesothelioma. *Curr Treat Options Oncol* 2002; **3**: 369–73.

10 Kafiri G, Thomas DM, Shepherd NA, Krausz T, Lane DP, Hall PA. p53 expression is common in malignant mesothelioma. *Histopathology* 1992; **21**: 331–34.

11 Hasteh F, Lin GY, Weidner N, Michael CW. The use of immunohistochemistry to distinguish reactive mesothelial cells from malignant mesothelioma in cytologic effusions. *Cancer Cytopathol* 2010; **118**: 90–96.

12 Gonz lez-Moreno S, Yan H, Alcorn KW, Sugarbaker PH. Malignant transformation of 'benign' cystic mesothelioma of the peritoneum. *J Surg Oncol* 2002; **79**: 243–51.

13 Minato H, Nojima T, Kurose N, Kinoshita E. Adenomatoid tumor of the pleura. *Pathol Int* 2009; **59**: 567–71.

Human Pathology (2011) 42, 1576–1579

ELSEVIER

Human
PATHOLOGY

www.elsevier.com/locate/humpath

Case study

Pleural cavity angiosarcoma arising in chronic expanding hematoma after pneumonectomy

Hideki Miyazaki MD[a], Akiteru Goto MD, PhD[a], Rumi Hino MD, PhD[a], Satoshi Ota MD, PhD[a], Reiko Okudaira MD, PhD[b], Tomohiro Murakawa MD, PhD[c], Jun Nakajima MD, PhD[c], Masashi Fukayama MD, PhD[a,*]

[a]*Department of Human Pathology, Graduate School of Medicine, The University of Tokyo, Hongo 7-3-1, Bunkyo-ku, Tokyo 113-0033, Japan*
[b]*Department of Respiratory Medicine, Graduate School of Medicine, The University of Tokyo, Hongo 7-3-1, Bunkyo-ku, Tokyo 113-0033, Japan*
[c]*Department of Thoracic Surgery, Graduate School of Medicine, The University of Tokyo, Hongo 7-3-1, Bunkyo-ku, Tokyo 113-0033, Japan*

Received 10 June 2010; revised 16 June 2010; accepted 16 June 2010

Keywords:
Angiosarcoma;
Chronic expanding hematoma;
Chest

Summary A 52-year-old man received a left pneumonectomy for pulmonary squamous cell carcinoma without signs of recurrence after surgery. At age 68 years, a capsulated huge mass developed in the left pleural cavity, which was diagnosed as chronic expanding hematoma. Two years and 8 months after detection, the lesion began to invade the chest wall, and 10 months later, the patient died of active bleeding and direct compression of the heart by the lesion. At autopsy, the left thoracic cavity was occupied by a cystic and hemorrhagic mass infiltrating into the surrounding structures. In addition, scattered tumorous nodules were observed in the right lung. Histologically, angiosarcoma with irregularly anastomosing vessels lined with atypical endothelial cells was noted in the chronic expanding hematoma. The final diagnosis was pleural cavity angiosarcoma arising in chronic expanding hematoma and its metastases to the right lung.

1. Introduction

Angiosarcoma (AS) is a relatively rare soft tissue tumor, accounting for less than 1% of all sarcomas [1]. It usually occurs on the face and scalp, deep soft tissue, liver, spleen, and breast. Pleural cavity AS is extremely rare and is reported to have strong linkage with chronic pyothorax, especially in Japanese patients [2]. Almost all of the AS cases complicated with pyothorax are associated with tuberculous pyothorax or a history of thoracoplasty for tuberculosis.

Chronic expanding hematoma (CEH) is a rare nonneoplastic reactive process, and it usually appears as a slowly growing hematoma [3]. CEH grows supposedly because unresolved initial hematoma leads to repeated organization and hemorrhage from new fragile microvessels. CEH can occur in various locations, including the chest [4]. CEH of the chest is considered a specific type of chronic empyema that occurs after thoracic injury, thoracic surgery, or tuberculous pleuritis.

* Corresponding author. Department of Human Pathology, Graduate School of Medicine, The University of Tokyo, Hongo 7-3-1, Bunkyo-ku, Tokyo 113-0033, Japan.
E-mail address: mfukayama-tky@umin.ac.jp (M. Fukayama).

0046-8177/$ – see front matter © 2011 Elsevier Inc. All rights reserved.
doi:10.1016/j.humpath.2010.06.019

Although CEH of the chest is an angioproliferative lesion and also classified as a form of chronic empyema, there are no English reports on AS associated with CEH to date. Here, the authors report a case of pleural cavity AS arising in CEH after pneumonectomy for lung cancer. CEH may be an unrecognized AS-prone feature of the chest.

2. Case report

2.1. Clinical summary

A 52-year-old Japanese man received a left pneumonectomy for pulmonary hilar cancer, pathologically diagnosed as well-differentiated squamous cell carcinoma. According to the TNM staging system (7th edition, International Union against Cancer) [5], the tumor was staged as pT3N1M0, stage IIb. He underwent adjuvant chemotherapy with cisplatin and vindesine, and no recurrence of the cancer was detected for 17 years (Fig. 1A). Preoperative or postoperative irradiation was not performed.

At the age of 68 years, he was referred to our hospital complaining of hoarseness. Chest computed tomographic (CT) scan revealed a capsulated large mass in the left pleural cavity, compressing the descending aorta (Fig. 1B). Bronchoscopy, positron emission tomography, and gallium scintigraphy showed no signs of malignancy. CT-guided needle biopsy was performed, only to aspirate bloody fluid containing no malignant cells. Culture of this specimen revealed no bacterium. The mass was considered to be a so-called CEH.

The size of the mass gradually increased, and the patient's laboratory data showed continuous C-reactive protein elevation (5-10 mg/dL), which was consistent of the course of CEH. However, 2 years and 8 months after diagnosis, the CEH began to invade the chest wall with osteolytic changes in the ribs (Fig. 1C). Needle biopsies

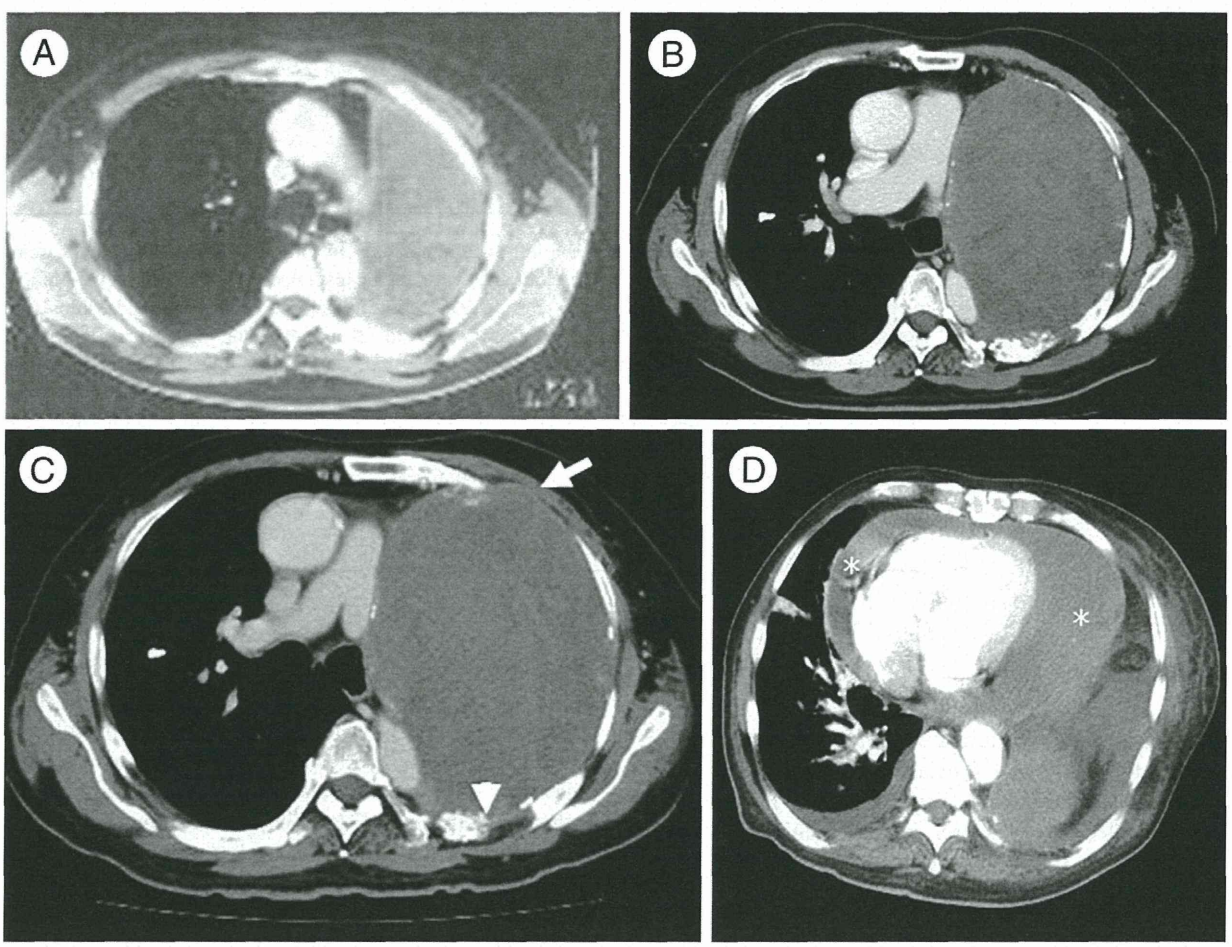

Fig. 1 A, Chest CT scan taken 8 years after left pneumonectomy. Left thoracic space shows soft tissue attenuation without signs of cancer recurrence. B, Chest CT scan taken 17 years after left pneumonectomy. A huge mass is occupying the left hemithorax and compressing the descending aorta. Compared with A, its growth is apparent. The CT findings are compatible with those of CEH. C, Two years and 8 months after the first detection of CEH. In addition to similar findings as B, invasion to the chest wall (arrow) and osteolytic change (arrow head) is observed. D, Just before the patient's death. The heart is directly surrounded and compressed by the lesion (*).

were performed twice, and both were unsuccessful in obtaining enough tissue to evaluate.

Although the possibility of malignant tumor was suspected, surgical treatment was not an option because of the patient's unstable condition. Ten months later, the patient died as a result of the heart being directly compressed by the lesion and the inability to arrest the active bleeding into the cystic cavity (Fig. 1D). An autopsy was performed 2 hours and 32 minutes after his death, with his family's consent.

2.2. Autopsy findings

Grossly, a 38 × 18 × 12 cm–sized mass with a central cavity containing necrotic and coagulative contents occupied the entire left thoracic cavity. The wall of the lesion was ill demarcated and strongly adherent and infiltrative to the surrounding structures such as mediastinal fat tissue, pericardial space, and myocardium. The mass was also infiltrative to the chest wall, destroying the fourth and fifth ribs and extending to the subcutaneous space.

Histologically, the central cavity was circumscribed by hyalinized fibrosis and hyperplastic microvessels without atypia, indicative of preexisting CEH (Fig. 2A and B). Such CEH histology was further encircled and partly intermingled with irregular anastomosing vascular channels of AS, lined by atypical endothelial cells (Fig. 2A and C). Most of the tumor cells of AS showed an epithelioid shape compared with the endothelial cells of the CEH. Immunohistochemical analysis was performed with antibodies against CD31 (JC/70A, dilution 1:40; Dako Corp, Grustrup, Denmark), CD34 (QBEND10, 1:400; Dako), Factor VIII-RA (F8/86, 1:700; Dako), CEA (carcinoembrionic antigen) (II-7, 1:200; Dako), cytokeratin (AE1/AE3, 1:200; Dako), EMA (epithelial membrane antigen) (E29, 1:200; Dako), calretinin (5A5, 1:50; Novocastra, Necastle upon Tyne, UK), P53 (DO-1, 1:250; Immunotech, Marseille, France), and Ki-67 (MIB-1, 1:200; Immunotech). The immunohistochemical results are summarized in Table 1. AS cells were strongly positive for CD31, and the immunoreactivity was limited for CD31 (in contrast to CEH microvessels and nondiseased vessels) (Fig. 2D). AS cells were negative for carletinin, CEA, and

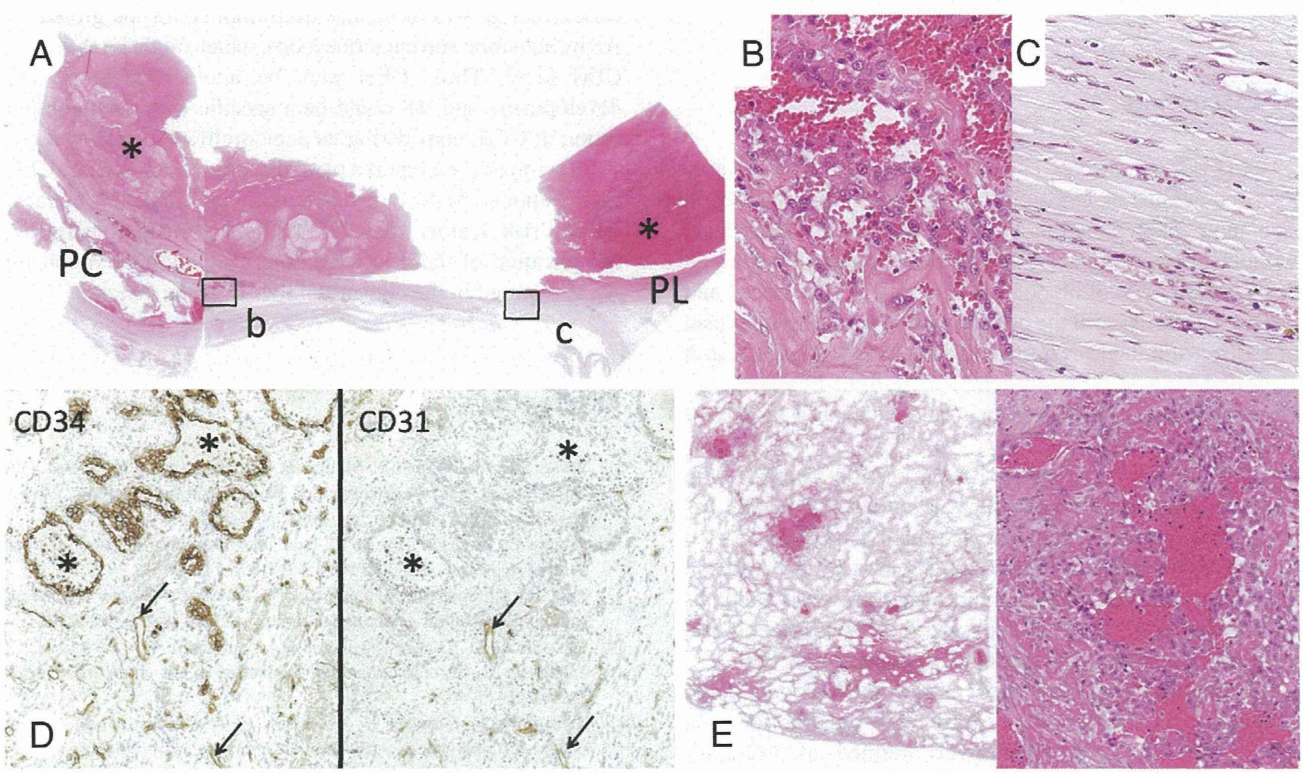

Fig. 2 A, Semimicroscopic view of the left thorax of the case. Pleura is fibrously thickened with coagula (*) inside. The hemorrhagic and vascular lesion is infiltrating to adjacent pericardium at the left lower corner of the figure, which corresponds to AS histologically (b) on the background of CEH (c). PL indicates pleura; PC, pericardium. B, Higher magnification of rectangular (b) area in A. Irregularly anastomosing microvessels were observed with hyperemia and hemorrhage. The endothelial cells showed cellular atypia with epithelioid features, which was suggestive of the diagnosis of AS. Higher magnification of rectangular (c) area in A. Proliferation of microvessels without atypia is seen, and the histology is compatible with that of CEH. C, Higher magnification of rectangular (c) area in A. Proliferation of microvessels without atypia is seen, and the histology is compatible with that of CEH. D, CD34 is strongly positive for AS vessels (*) and for surrounding CEH vessels (arrow). Immunoreactivity of AS (*) vessels for CD31 is weaker than for CEH vessels (arrow). E, The lung parenchyma shows numerous tumorous nodules (left). At higher magnification, atypical endothelial cells of AS are observed forming anomalous microvessels (right).

Table 1 Summary of the results for immunohistochemical analysis of the case

Antibody	AS	CEH vessels	Normal vessels
CD31	+++	+++	+++
CD34	+	+++	+++
Factor VIII-RA	++	+++	+++
CEA	−	−	−
AE1/AE3	−	−	−
EMA	−	−	−
Calretinin	−	−	−
P53	+	+	−
Ki-67	++	++	+

+++ indicates 67% to 100% positive; ++, 33% to 66% positive; +, 1% to 33% positive; −, negative.

EMA, and no abnormal accumulation of p53 was observed (Table 1). The overall pathologic features were diagnostic of a pleural cavity AS arising in CEH.

The right lung had metastatic AS (Fig. 2E), and no recurrence of the left lung squamous cell carcinoma was identified at autopsy.

3. Discussion

CEH is a rare disease entity first advocated by Reid et al [3]. It is defined as hematoma that persists and increases in size more than a month after the initiating hemorrhage, without histologic neoplasm and hemorrhagic diathesis. It has a central mass of blood; a wall of granulation tissue; and dense, fibrous tissue at the periphery. The growth mechanism of CEH is still unclear, but some authors hypothesize that it grows because of repeated hemorrhage from fragile microvessels formed in inflammation, which is caused by a prior hemorrhage [3,4].

In the present case, AS did not presumably coincide with the first detection of thoracic mass lesion, as AS usually has an ominous prognosis and patients seldom survive the period of more than 3 years as in this case [1]. In addition, invasion to the chest wall radiologically appeared 2 years and 8 months after detection of the mass. Considering this clinical course, it is conceivable that AS developed in preexisting CEH.

Differential diagnosis of CEH and AS is a histopathologic challenge, as both show endothelial proliferation. In fact, CEH has been alternatively termed as *Masson's pseudoangiosarcoma* or *extravascular papillary endothelial hyperplasia*, focusing on its angioproliferative features [6]. In the present case, endothelial atypia was noted only in AS lesions, including its metastases in the right lung, and an epithelioid appearance was observed in the AS cells. In addition, AS of the present case showed differential expression for CD31 and CD34. AS vessels were strongly and diffusely positive for CD31, whereas its positivity was limited for CD31, in contrast to the background CEH vessels. Although comparative study of CD31 and CD34 expressions has not been extensively performed between AS and nonmalignant vascular lesions, Rossi and Fletcher [7] implicated greater positivity for CD34 than CD31 in AS through their study of AS arising in hemangioma/vascular malformation. Thus, the combination of CD34 and CD31 immunohistochemistry was helpful in distinguishing AS from CEH in the present case. We also used p53 immunohistochemistry, as abnormal nuclear accumulation of p53 has been reported in 20% of AS cases [8]. However, AS in the present case showed only scattered staining in less than 5% of the cells, and p53 was not useful in distinguishing AS from background CEH. In addition, the MIB-1 labeling index did not significantly differ between AS and CEH.

Pleural cavity AS is an extremely rare disease accounting for only 6% of all ASs in a Japanese review study [2]. Interestingly, all of the pleural cavity AS cases in that series were complicated with pyothorax related to tuberculosis. Thus far, AS developing in CEH has not been reported in the English literature. However, the inflammatory background seen in chronic tuberculous pyothorax and CEH may play a role in AS development. In addition, the involvement of vascular endothelial growth factor has been implied for the growth of AS by autocrine and paracrine loops, which might be shared by CEH [1,9]. Thus, CEH may be another cause of AS development, and AS could be a specific malignant complication of CEH, considering its angioproliferative features.

In summary, we report a pleural cavity AS arising in a CEH case without a history of tuberculosis and radiation therapy, known risk factors for AS. AS is a potential malignant complication of thoracic CEH, and cautious observation for AS is required in the clinical follow-up of the disease.

References

[1] Weiss SW, Goldblum JR. Malignant vascular tumors. In: Weiss SW, Goldblum JR, editors. Enzinger and Weiss's soft tissue tumors. 5th ed. Philadelphia (PA): Mosby Inc; 2008. p. 703-32.
[2] Aozasa K, Naka N, Tomita Y, et al. Angiosarcoma developing from chronic pyothorax. Mod Pathol 1994;7:906-11.
[3] Reid JD, Kommareddi S, Lankerani M, Park MC. Chronic expanding hematomas. A clinicopathological entity. JAMA 1980;224:2441-2.
[4] Kuronuma K, Ootake S, Ikeda K, Taniguchi M, Takezawa C, Takahashi H. Chronic expanding hematoma in the chest. Intern Med 2008;47:1411-4.
[5] Rami-Porta R, Crowley JJ, Goldstraw P. The revised TNM staging system for lung cancer. Ann Thorac Cardiovasc Surg 2009;15:4-9.
[6] Duarte IG, Chang HJ, Kennedy JC, Miller Jr JI. Papillary endothelial hyperplasia presenting as a chest wall neoplasm. Ann Thorac Surg 1999;67:238-40.
[7] Rossi S, Fletcher CD. Angiosarcoma arising in hemangioma/vascular malformation: report of four cases and review of the literature. Am J Surg Pathol 2002;26:1319-29.
[8] Meis-Kindblom JM, Kindblom LG. Angiosarcoma of soft tissue: a study of 80 cases. Am J Surg Pathol 1998;22:683-97.
[9] Tokuyama W, Mikami T, Masuzawa M, Okayasu I. Autocrine and paracrine roles of VEGF/VEGFR-2 and VEGF-C/VEGFR-3 signaling in angiosarcomas of the scalp and face. Hum Pathol 2010;41:407-14.